Effect of MgO concentration on phase evolution during steelmaking slag cooling process

W.F. Gu [1], *J. Diao* *[2], *H. Qin* [3], *H.F. Yu* [4], *Y. Sasaki* [5], *S. Ueda* [6]

1. Doctoral candidate, Chongqing University, College of Materials Science and Engineering, and Tohoku University, Institute of Multidisciplinary Research for Advanced Materials, 400044. Email:guwengfeng@163.com
2. Associate professor, Chongqing University, College of Materials Science and Engineering, 400044. Email: diaojiang@163.com
3. Master candidate, Chongqing University, College of Materials Science and Engineering, 400044. Email: qh1240980784@163.com
4. Associate professor, University of Science and Technology Beijing, State Key Laboratory of Advanced Metallurgy, 100083. Email: yuhuafang@ustb.edu.cn
5. Professor, Tohoku University, Institute of Multidisciplinary Research for Advanced Materials, 980-0812. Email: ironyaz@gmail.com
6. Professor, Tohoku University, Institute of Multidisciplinary Research for Advanced Materials, 980-0812. Email: shigeru.ueda.a5@tohoku.ac.jp

Keywords: Steelmaking slag, MgO, Phase evolution, Instability, Ca_3SiO_5

ABSTRACT

The main reason for the underutilization of steelmaking slags is their instability, which is influenced by their complex phase structure. Recycling and sustainable steelmaking slag face challenges due to the presence of magnesium oxide (MgO), a crucial component in steelmaking slag. This study investigates the phase evolution of steelmaking slag during the cooling process with different MgO contents, using high-temperature experiments and FactSage thermodynamic equilibrium calculations. XRD and SEM-EDS analyses identified main phases in steelmaking slag, including Ca_2SiO_4 (C_2S), RO (MgO-FeO solid solution), $Ca_2Fe_2O_5$ (C_2F), and Ca_3SiO_5 (C_3S). The study reveals that RO phase increases as the MgO content increases. C_3S precipitates from steelmaking slag with a 12 mass% MgO content at a reduced temperature of 1400°C. It is important to note that C_3S remains in the steelmaking slag even after slow cooling. This may be due to the substitution of Ca^{2+} in C_3S by Fe^{2+} and Mg^{2+} ions. Intriguingly, the precipitation of *f*-CaO in steelmaking slag with 10 mass% of MgO content occurred after one year, while there was no manifestation of *f*-CaO precipitation in the steelmaking slag with 12 mass% of MgO content even after one year. This discrepancy suggests a potential stabilizing effect of an appropriate amount of MgO in steelmaking slag. However, it is crucial to emphasize that this inference lacks supporting data, necessitating further research to validate this hypothesis. The significance of this work is in uncovering the complexities of steelmaking slag behavior, providing essential insights for optimizing recycling processes. The research sheds light on the factors that influence the phase composition and stability of steelmaking slag, contributing to the utilization of steelmaking slags, promoting environmental sustainability, and enhancing the overall efficiency of metallurgical processes in the current industrial landscape.

INTRODUCTION

In China, the steel industry annually generates a substantial 130-160 million tons of steelmaking slag, yet its utilization rate is less than 30%(Carvalho et al., 2017; Guo et al., 2018; Oge et al., 2019). Utilizing steelmaking slag in building materials can alleviate disposal challenges and reduce reliance on natural resources. However, its application has been hindered by characteristics such as volume expansion during storage(Park et al., 2019; Ruan et al., 2022; Zhao et al., 2017). The expansion in volume is attributed to the hydration of free lime (*f*-CaO) and dusting resulting from the conversion of α'-Ca_2SiO_4 (α'-C_2S) to γ-Ca_2SiO_4 (γ-C_2S) within the slag(Benarchid et al., 2005; Brand and Roesler, 2018).

A comprehensive understanding of the chemical, mineralogical, and morphological properties of steelmaking slag is crucial, as these properties directly impact its cementitious and mechanical attributes, influencing its utilization potential. Given the significant variability in chemical composition among different sources of steelmaking slag, substantial differences in mineralogical composition are expected(Deng et al., 2020; Kim and Azimi, 2022; Shen et al., 2004; Yu et al., 2022). To enhance steel/slag reactions and dephosphorization kinetics during the steelmaking process, considerable amounts of dolomite are introduced into the converter (Tayeb et al., 2015). The addition of dolomite, coupled with the loss of MgO refractory in the BOF lining, results in a slag containing 0.4-14% MgO, resulting in a stability issue for steelmaking slag (Yildirim and Prezzi, 2011).

The decomposition of Ca_3SiO_5 (C_3S) during the cooling process of steelmaking slag is a major source of *f*-CaO(Li et al., 2022; Shim et al., 2016; Tossavainen et al., 2007). However, Ca_3SiO_5 is also a vital component in Portland cement clinker. Consequently, the stability steelmaking slag directly influences its suitability for civil engineering and building materials. Research indicates that MgO content affects the crystal structure of C_3S, with low MgO stabilizing the triclinic polymorph, while high MgO favors the formation of the monoclinic(Chen et al., 2014; Liu et al., 2002; Ma et al., 2015). This study investigates the phase evolution of steelmaking slag with varying MgO content during the cooling process, employing thermodynamic equilibrium phase calculations and molten steelmaking slag cooling experiments. The aim is to understand the influence of MgO content on the formation of phases and stability, optimizing the mineral phase of steelmaking slag and enhancing its stability. This research will contribute a theoretical foundation for the treatment of steelmaking slag.

MATERIALS AND METHODS

Steelmaking slags with different magnesium oxide (MgO) contents were prepared using analytical reagents, and their chemical composition is detailed in TABLE 1. The raw mixtures, weighing 40 g, were dried and then subjected to burning at 1500°C for 40 minutes. The temperature decrease occurred at a rate of 5°C/min, as shown in FIG 1. After the sample reached the target temperature, a connected quartz tube and pipette are used to extract the steelmaking slag sample for analysis of the precipitate phases during the steelmaking slag cooling process. Upon reaching 1000°C, the molten steelmaking slag had completely solidified. Subsequently, the slags were cooled to room temperature at a rate of 30°C/min. The experimental process was conducted under an argon (Ar) atmosphere to prevent the oxidation of the steelmaking slag, and all samples were rapidly cooled with water. The phases and microstructure of slag samples were analyzed by scanning electron microscopy, SEM-EDS, (VEGA 3 LMH, TESCAN, Brno, Czech) and X-ray diffraction (PANalytical X'Pert Power, PANalytical B.V., Netherlands).

TABLE 1. Chemical compositions of steelmaking slags (mass%)

No.	MgO	CaO	Fe_xO	SiO_2	Al_2O_3	P_2O_5	MnO	TiO_2
1	8.00	44.53	28.63	12.72	2.04	2.04	1.02	1.02
2	10.00	43.56	28.00	12.44	2.00	2.00	1.00	1.00
3	12.00	42.59	27.37	12.16	1.96	1.96	0.98	0.98

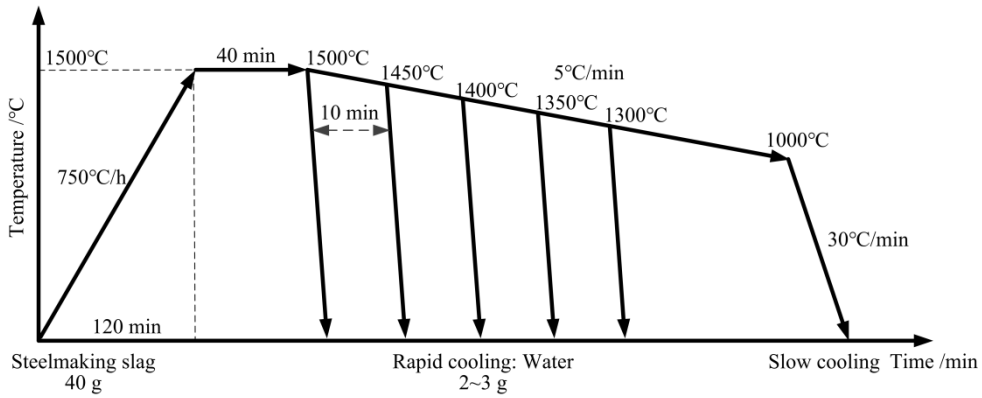

FIG 1 –.Scheme of the heat patterns in this experiment

RESULT AND DISCUSSION

Equilibrium phase of steelmaking slag

The thermodynamic equilibrium calculation results depicted in FIG 2 illustrate the predominant phases in steelmaking slags with 8 mass% and 12 mass% MgO. These phases encompass RO, C_2S, C_3S, C_2S-C_3P (solid solution of Ca_2SiO_4 and $Ca_3(PO_4)_2$), C_2F, and *f*-CaO. Notably, RO emerges as the initial precipitation phase in molten steelmaking slag, with its content at 1600°C escalating from 5.46 mass% to 10.91 mass% with an increase in MgO content from 8 mass% to 12 mass%. Correspondingly, the RO contents in fully solidified steelmaking slag exhibit a range of 35.84 mass% to 38.32 mass%. The findings in the figure unequivocally establish the RO phase as the exclusive form of MgO post-solidification of the steelmaking slag.

As shown in FIG 2, the increase of MgO content results in a reduction of the liquid phase in molten steelmaking slag. Consequently, there is an elevation in the concentration of CaO in the liquid phase, facilitating the precipitation of C_3S. At an MgO content of 8 mass%, C_3S precipitates in the steelmaking slag at 1375°C. With a further increase in MgO content to 12 mass%, the precipitation temperature of C_3S rises to 1405°C. As the temperature decreases, the C_3S content increases to 7.50 mass% and 12.19 mass%, respectively, before ultimately decomposing into C_2S and *f*-CaO at

1300°C. The data in FIG 2 conclusively suggests that the increasing in MgO content does not exert a significant influence on the *f*-CaO content in steelmaking slag.

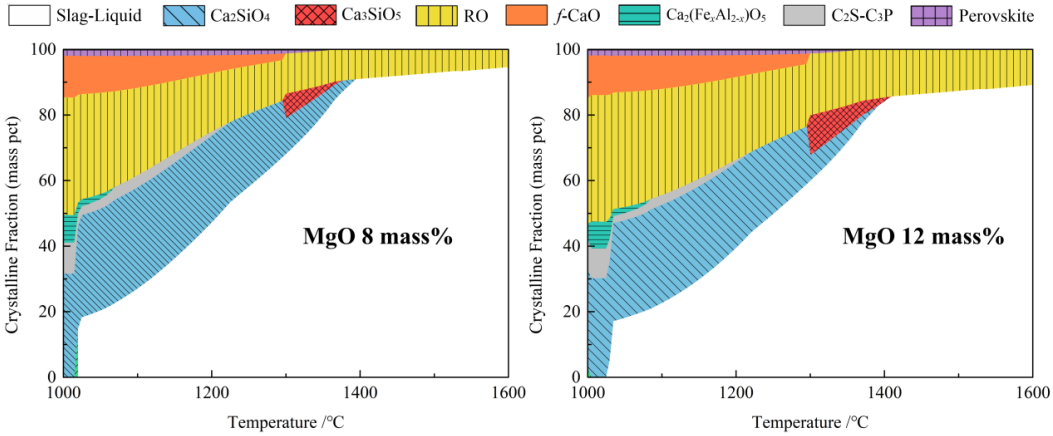

FIG 2 – Thermodynamic calculation based on a normal equilibrium calculation model for steelmaking slag with different MgO content. Fe_2O_3 content is 10 mass% of iron oxides in all steelmaking slags.

Mineral phase structure

The XRD patterns for steelmaking slags containing 12 mass% MgO at different temperatures are depicted in FIG 3. It can be deduced that the primary phases in the steelmaking slag include C_2S, RO, C_2F, and C_3S. FIG 3 illustrates the precipitation of C_3S from the steelmaking slag with 12 mass% MgO content at a reduced temperature of 1400°C.

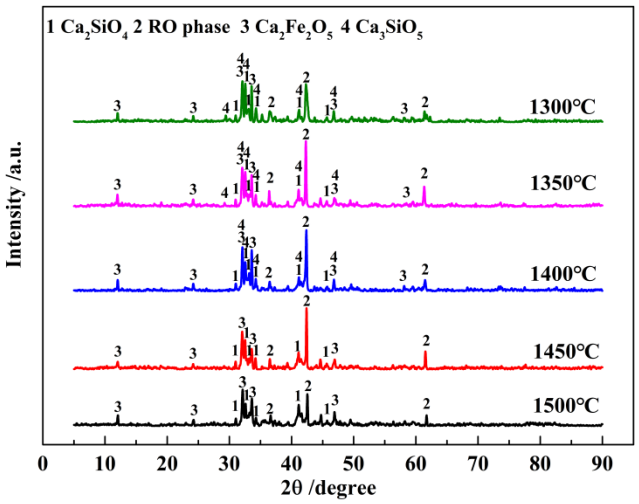

FIG 3 – XRD patterns of steelmaking slags of 12 mass% MgO during cooling

FIG 4 displays SEM images of slowly cooling steelmaking slag with different MgO contents, revealing C_3S in bulk structures. Interestingly, the increase in MgO content has an insignificant impact on the composition and phases of the steelmaking slag. After cooling, steelmaking slag maintains phases such as C_2S, RO, C_2F, and C_3S, with no precipitation of C_3S in the case of 8 mass% MgO content. The persistence of C_3S in steelmaking slag after slow cooling, as observed, indicates that, under the experimental conditions, the kinetics required for the decomposition of C_3S have not been achieved.

As shown in FIG 4, EDS results demonstrate the presence of Mg and Fe in C_3S, suggesting the possibility of Fe^{2+} and Mg^{2+} substituting for Ca^{2+} in the C_3S crystal lattice. Notably, Mg serves not only as a substitutional atom but also as an interstitial atom. The addition of an appropriate amount of MgO to steelmaking slag has the potential to alter the formation kinetics of C_3S, influencing its crystal structure.

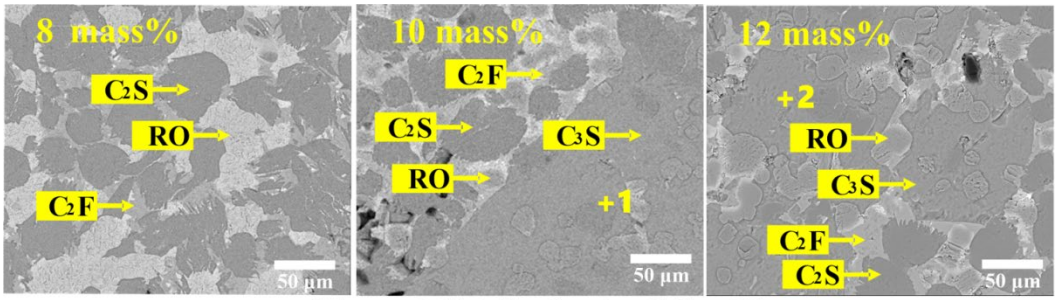

Element distribution in C_3S, at%

No.	O	Mg	Si	Ca	Fe
1	65.2	0.5	7.1	25.1	2.2
2	53.1	0.7	11.8	32.1	2.3

FIG 4 – SEM of the slowly cooled steelmaking slags with different MgO mass% (The table shows the EDS results for points 1 and 2 in the figure)

Stability of steelmaking slag

As already mentioned, steelmaking slag has been of limited use due to its characteristics of volume expansion during storage. The volume expansion is caused by the hydration of free lime (f-CaO) in the slag, which exhibits around 10 % swelling (Bazzoni et al., 2014; Stephan and Wistuba, 2006). Samples were polished and placed in air to investigate the stability of steelmaking slag at room temperature. The steelmaking slag surface starts to precipitate some black phase, as shown in FIG 5. Based on the SEM-EDS results in FIG 6, the black phase is considered to be gradually precipitated *f*-CaO. As shown in FIG 5 and FIG 6, the MgO in the slag was 10 mass% and a large amount of *f*-CaO precipitated from the slag surface after one year. However, when the MgO content was increased to 12 mass%, there was no significant change in slag surface after one year. It suggests a potential stabilizing effect of an appropriate amount of MgO in steelmaking slag. Nevertheless, it is crucial to emphasize that this inference lacks empirical support, and additional studies are imperative to validate this hypothesis and provide a more comprehensive understanding of the underlying mechanisms.

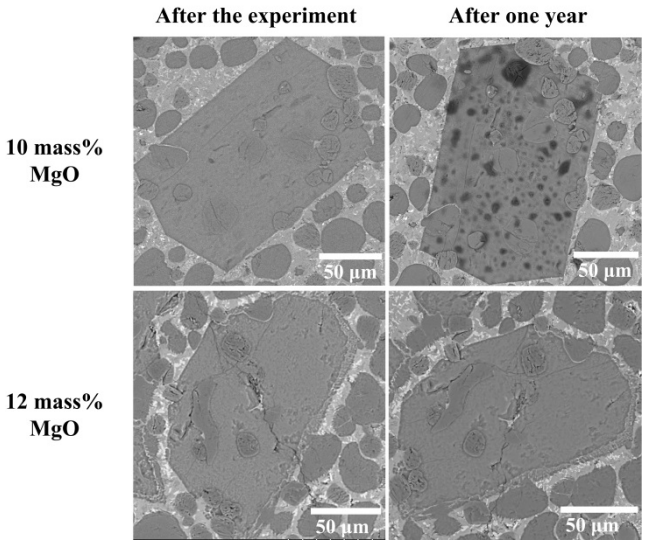

FIG 5 – SEM of steelmaking slag after one year for different MgO contents

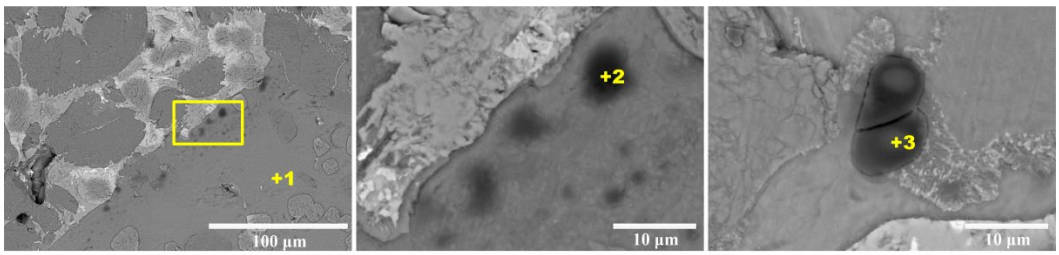

EDS result of slag with 10 mass% MgO, at%

NO.	O	Mg	Si	Ca	Fe	Ca/Si
1	61.38	0.57	7.37	28.62	2.06	3.88
2	68.14	0.87	5.05	23.55	2.39	4.66
3	77.33	0.81	1.90	18.30	1.65	9.63

FIG 6 – SEM and EDS of steelmaking slag with 10 mass% MgO after one year

CONCLUSIONS

The investigation systematically examined the evolution of mineral phases and microstructures during the cooling of steelmaking slag with varying MgO contents, aiming to enhance the efficient recycling of steelmaking by-products. The principal findings are outlined as follows: the dominant phases in steelmaking slag encompass C_2S, RO, C_2F and C_3S. RO phase, representing the main form of MgO in steelmaking slag, exhibited an increase from 35.84 mass% to 38.32 mass% with the MgO content rising from 8 mass% to 12 mass%. Simultaneously, an increasing in MgO content also heightened the C_3S precipitation content in steelmaking slag. Cooling experiments revealed that C_3S in steelmaking slag did not decompose into C_2S and CaO with decreasing temperature, possibly attributed to the ability of certain Fe^{2+} and Mg^{2+} to substitute Ca^{2+} in C_3S. Interestingly, the precipitation of *f*-CaO in steelmaking slag with 10 mass% of MgO content occurred after one year, while the precipitation of *f*-CaO in steelmaking slag with 12 mass% of MgO content did not manifest even after one year. This discrepancy implies a potential stabilizing effect of an appropriate amount of MgO in steelmaking slag. However, it is essential to note that this inference lacks supporting data, and further research is required to validate this hypothesis.

REFERENCES

Bazzoni, A., Ma, S., Wang, Q., Shen, X., Cantoni, M., and Scrivener, K. L. (2014). The Effect of Magnesium and Zinc Ions on the Hydration Kinetics of C 3 S. Journal of the American Ceramic Society, 97(11), 3684–3693. https://doi.org/10.1111/jace.13156

Benarchid, My. Y., Diouri, A., Boukhari, A., Aride, J., and Elkhadiri, I. (2005). Hydration of iron–phosphorus doped dicalcium silicate phase. Materials Chemistry and Physics, 94(2–3), 190–194. https://doi.org/10.1016/j.matchemphys.2005.04.047

Brand, A. S., and Roesler, J. R. (2018). Interfacial transition zone of cement composites with steel furnace slag aggregates. Cement and Concrete Composites, 86, 117–129. https://doi.org/10.1016/j.cemconcomp.2017.11.012

Carvalho, S. Z., Vernilli, F., Almeida, B., Demarco, M., and Silva, S. N. (2017). The recycling effect of BOF slag in the portland cement properties. Resources, Conservation and Recycling, 127, 216–220. https://doi.org/10.1016/j.resconrec.2017.08.021

Chen, L., Wang, X., Shen, X. D., Ma, S. H., and Zhou, W. Q. (2014). Crystal Structure and Hydration Characteristics of Tricalcium Silicate Doped with Magnesium Oxide. Advanced Materials Research, 936, 1336–1341. https://doi.org/10.4028/www.scientific.net/AMR.936.1336

Deng, L., Yun, F., Jia, R., Li, H., Jia, X., Shi, Y., and Zhang, X. (2020). Effect of SiO2/MgO ratio on the crystallization behavior, structure, and properties of wollastonite-augite glass-ceramics derived from stainless steel slag. Materials Chemistry and Physics, 239, 122039. https://doi.org/10.1016/j.matchemphys.2019.122039

Fix, W., Heymann, H., and Heinke, R. (n.d.). Subsolidus Relations in the System 2CaO SiO2 -3Ca0 Y 2 05.

Guo, J., Bao, Y., and Wang, M. (2018). Steel slag in China: Treatment, recycling, and management. Waste Management, 78, 318–330. https://doi.org/10.1016/j.wasman.2018.04.045

Kim, J., and Azimi, G. (2022). Selective Precipitation of Titanium, Magnesium, and Aluminum from the Steelmaking Slag Leach Liquor. Resources, Conservation and Recycling, 180, 106177. https://doi.org/10.1016/j.resconrec.2022.106177

Li, Y., Guo, K., Xiang, J., Pei, G., and Lv, X. (2022). Effect of Cooling Method on the Mineralogy and Stability of Steel Slag. ISIJ International, 62(11), 2197–2206. https://doi.org/10.2355/isijinternational.ISIJINT-2022-101

Liu, X., Li, Y., and Zhang, N. (2002). Inf luence of MgO on the formation of Ca3SiO5 and 3CaOÁ3Al2O3ÁCaSO4 minerals in alite–sulphoaluminate cement. Cement and Concrete Research.

Ma, S., Zhou, W., Wang, S., Li, W., and Shen, X. (2015). Polymorph transformation kinetics of Ca 3 SiO 5 with MgO. Phase Transitions, 88(9), 888–896. https://doi.org/10.1080/01411594.2015.1030746

Oge, M., Ozkan, D., Celik, M. B., Sabri Gok, M., and Cahit Karaoglanli, A. (2019). An Overview of Utilization of Blast Furnace and Steelmaking Slag in Various Applications. Materials Today: Proceedings, 11, 516–525. https://doi.org/10.1016/j.matpr.2019.01.023

Park, T. J., Choi, J. S., and Min, D. J. (2019). Investigation of Effects of SiO2 Content and Cooling Rate on Crystallization in Fe2O3-CaO-SiO2 System Using In Situ Confocal Laser Scanning Microscopy. Metallurgical and Materials Transactions B, 50(2), 790–798. https://doi.org/10.1007/s11663-019-01518-y

Ruan, W., Ma, Y., Liao, J., Ma, T., Zhu, Y., and Zhou, A. (2022). Effects of steel slag on the microstructure and mechanical properties of magnesium phosphate cement. Journal of Building Engineering, 49, 104120. https://doi.org/10.1016/j.jobe.2022.104120

Shen, H., Forssberg, E., and Nordström, U. (2004). Physicochemical and mineralogical properties of stainless steel slags oriented to metal recovery. Resources, Conservation and Recycling, 40(3), 245–271. https://doi.org/10.1016/S0921-3449(03)00072-7

Shi, C., Inc, C. T., Dr, U., and On, B. (n.d.). Steel Slag—Its Production, Processing, Characteristics, and Cementitious Properties.

Shim, G.-I., Kim, S.-H., Paik, D.-J., Hong, M.-H., and Choi, S.-Y. (2016). Influence of cooling rate on the crushing efficiency of solidified iron ore for recycled aggregates. International Journal of Mineral Processing, 150, 9–15. https://doi.org/10.1016/j.minpro.2016.03.002

Stephan, D., and Wistuba, S. (2006). Crystal structure refinement and hydration behaviour of 3CaO·SiO2 solid solutions with MgO, Al2O3 and Fe2O3. Journal of the European Ceramic Society, 26(1–2), 141–148. https://doi.org/10.1016/j.jeurceramsoc.2004.10.031

Tayeb, M. A., Assis, A. N., Sridhar, S., and Fruehan, R. J. (2015). MgO Solubility in Steelmaking Slags. Metallurgical and Materials Transactions B, 46(3), 1112–1114. https://doi.org/10.1007/s11663-015-0352-8

Tossavainen, M., Engstrom, F., Yang, Q., Menad, N., Lidstrom Larsson, M., and Bjorkman, B. (2007). Characteristics of steel slag under different cooling conditions. Waste Management, 27(10), 1335–1344. https://doi.org/10.1016/j.wasman.2006.08.002

Yildirim, I. Z., and Prezzi, M. (2011). Chemical, Mineralogical, and Morphological Properties of Steel Slag. Advances in Civil Engineering, 2011, 1–13. https://doi.org/10.1155/2011/463638

Yu, H., Lu, X., Miki, T., Matsubae, K., Sasaki, Y., and Nagasaka, T. (2022). Sustainable phosphorus supply by phosphorus recovery from steelmaking slag: A critical review. Resources, Conservation and Recycling, 180, 106203. https://doi.org/10.1016/j.resconrec.2022.106203

Zhao, J., Yan, P., and Wang, D. (2017). Research on mineral characteristics of converter steel slag and its comprehensive utilization of internal and external recycle. Journal of Cleaner Production, 156, 50–61. https://doi.org/10.1016/j.jclepro.2017.04.029